

See discussions, stats, and author profiles for this publication at: <https://www.researchgate.net/publication/231684456>

Effect of crosslinks on the miscibility of a deuterated polybutadiene and protonated polybutadiene blend

ARTICLE in *MACROMOLECULES* · JANUARY 1993

Impact Factor: 5.8 · DOI: 10.1021/ma00053a028

CITATIONS

11

READS

9

5 AUTHORS, INCLUDING:



Hiroshi Jinnai

Tohoku University

234 PUBLICATIONS 4,233 CITATIONS

SEE PROFILE



Hirokazu Hasegawa

Kyoto University

163 PUBLICATIONS 4,893 CITATIONS

SEE PROFILE



Takeji Hashimoto

Kyoto University

516 PUBLICATIONS 16,964 CITATIONS

SEE PROFILE



Robert M Briber

University of Maryland, College Park

151 PUBLICATIONS 2,502 CITATIONS

SEE PROFILE

Effect of Cross-Links on the Miscibility of a Deuterated Polybutadiene and Protonated Polybutadiene Blend

Hiroshi Jinnai, Hirokazu Hasegawa, and Takeji Hashimoto*

Department of Polymer Chemistry, Kyoto University, Kyoto 606-01, Japan

Robert M. Briber† and Charles C. Han

Polymers Division, National Institute of Standards and Technology,
Gaithersburg, Maryland 20899

Received May 27, 1992; Revised Manuscript Received September 17, 1992

ABSTRACT: The effect of peroxide cross-linking on the phase diagram and the scattering function for a critical mixture of perdeuterated polybutadiene (DPB) and protonated polybutadiene (HPB) has been examined by small-angle neutron scattering as a function of temperature. The scattering curves for the cross-linked blends were essentially temperature independent. It was found that even at temperatures (T) below the critical temperature (T_c) of the un-cross-linked (linear) blend (e.g., $T = 0^\circ\text{C}$; $T_c = 99.2^\circ\text{C}$), the cross-linked blends remained single phase and did not undergo microphase separation. The calculation of the reduced temperature, ϵ , for the cross-linked blends also implied that the cross-linking greatly increased the single-phase region of the phase diagram. A comparison of the scattering for the cross-linked blend with that of the linear blend at the cross-linking temperature (150°C) showed a suppression in the scattering due to the presence of the cross-links. However, it was experimentally found that the concentration fluctuations present at the temperature of cross-linking dominate the scattering, which made it rather difficult to verify the prediction on the scattering function made by de Gennes.

I. Introduction

It is extremely important to control the state of mixing and the phase-separated structure of polymer blends if they are to be designed to have superior properties relative to those of the individual constituent polymers. Phase-separated polymer blends with a well-controlled domain size and structure are favored for improving the physical properties in some cases,¹ while miscible blends are favored in other situations.² Small-angle neutron scattering (SANS) is a powerful technique to examine the concentration fluctuations present in polymer blends in the single-phase state as the spinodal is approached.³⁻⁷ Studies of these kind provide information on the magnitude of the Flory interaction parameter, χ , the spinodal temperature, T_s , and the correlation length of the system. These parameters are important when one attempts to judge the extent of miscibility of polymer blends. It has been shown in block copolymers both experimentally² and theoretically⁸ that coupling two dissimilar chains at a single junction increases the single-phase region of the phase diagram relative to that of a blend of the corresponding linear polymers. Briber and Bauer⁹ have demonstrated that introducing cross-links in a miscible polymer blend of deuterated polystyrene (DPS) and poly(vinyl methyl ether) (PVME) also increases the single-phase region of the phase diagram.

In this paper we studied the effect of cross-links on the concentration fluctuations in a deuterated polybutadiene (DPB) and protonated polybutadiene (HPB) blend. The effect of cross-links on the scattering was examined as a function of temperature and cross-link density. We experimentally found that the cross-linked blends remain single phase even at temperatures 100°C below T_s for the un-cross-linked blend. This observation suggests that introducing cross-links in the miscible blend greatly enhances the single-phase region of the phase diagram, which is consistent with the results reported by Briber

and Bauer and with prediction by de Gennes.²² However, unlike the observations by Briber and Bauer, the scattering from cross-linked blend in this paper did not agree with predictions by de Gennes.²² This can be understood if one considers a possibility that the concentration fluctuations which are present before cross-linking are "locked-in" by the cross-linking. In the DPB/HPB blends, these locked-in concentration fluctuations may dominate compared to those predicted by de Gennes at the experimentally accessible temperatures. The origin that caused the seemingly different observations between DPB/HPB blend and DPS/PVME blend is also discussed in detail.

II. Experimental Section

1. Samples. Both the perdeuterated polybutadiene (DPB) and the protonated polybutadiene (HPB) used in this study were synthesized by living anionic polymerization. Molecular weights and polydispersities of DPB and HPB are listed in Table I. The peroxide employed in this study for cross-linking of DPB and HPB was 1,1-bis(*tert*-butylperoxy)-3,3,5-trimethylcyclohexane. The half-life of the peroxide, $t_{1/2}$, for radical generation of this peroxide at 150°C is 66 s.¹⁰

Five DPB/HPB blend samples were made with a composition of 46.5 vol % DPB and 53.5 vol % HPB, containing 0, 2.57, 4.00, 5.52, and 8.51 wt % peroxide of the total polymer weight, respectively, to produce a series of samples with differing cross-link densities; 0.5 wt % *N*-phenyl-2-naphthylamine of the total polymer weight was added as an antioxidant. The composition was chosen so that the mixture had a critical volume fraction calculated according to Flory-Huggins lattice theory.¹¹ The SANS samples were prepared by dissolving the polymer mixture in cyclohexane and then freeze-drying. It should be noted that the DPB/HPB blend has an upper critical solution temperature (UCST) type phase diagram with a critical temperature of 99.2°C (see section III-2 for details).¹² Therefore, if one stores the mixture at room temperature for any length of time, the blend undergoes phase separation. Consequently, the mixture obtained after freeze-drying was homogenized by mechanical mixing¹³ at about 90°C and then molded into the spacer ring (1 mm in thickness and 14 mm in diameter) that would be used for the scattering experiment. The samples were sandwiched by two quartz plates and put in the brass SANS cell. The samples were kept at 105°C for 10 min, where the mixture was in the single-

* Present address: Department of Materials and Nuclear Engineering, University of Maryland, College Park, MD 20742-2155.

Table I
Polymer Characteristics

code (specimen)	$\bar{M}_n \times 10^{-4}$ ^a	\bar{M}_w/\bar{M}_n ^a	\bar{N}_n ^b	microstructure, ^c %		
				1,2	cis-1,4	trans-1,4
DPB	47.9	1.28	6223	21.5	36.3	42.2
HPB	28.9	1.06	5039	29.3		70.7

^a Determined by size exclusion chromatography equipped with light scattering. ^b Number-average degree of polymerization. ^c Determined by ¹³C NMR.

Table II
DPB/HPB Cross-Linked Blend Characteristics

peroxide concn, ^a wt %	swelling ratio (Q)	N_c	$q^* \times 10^2$, ^b Å ⁻¹	$q^* \times 10^2$, ^c Å ⁻¹
0			0	0
2.57	7.03	446	3.69	1.56
4.00	4.77	167	6.02	2.54
5.52	3.92	98	7.87	3.32
8.51	2.83	38	12.6	5.31

^a Peroxide concentration for total polymer weight. ^b Calculated from theoretical prediction by de Gennes (eq 8). ^c Calculated from experimentally determined value for DPS/PVME by Briber and Bauer (eq 9).

phase region of the phase diagram (see section III-2.) and no effective cross-linking reaction takes place, in order that all of the samples had the same concentration fluctuations before cross-linking. A temperature jump from 105 to 150 °C was made to decompose the peroxide and cross-link the samples. The blends were kept at 150 °C for 10 min, which was about 10 times the $t_{1/2}$. After the temperature jump, the disk-shaped cross-linked samples (except the one having 0 wt % peroxide) were removed from the SANS cell and placed in an excess of toluene and allowed to reach swelling equilibrium. The toluene was exchanged three or four times and allowed to reequilibrate to extract unreacted linear polymer or residual peroxide. At the end of this extraction process the diameter and the thickness of the disk-shaped samples were measured to calculate the swelling ratio of the cross-linked blend (see section II-2 for details). The samples were dried and then put back into the cells for the SANS measurements.

2. Characterization of Cross-Linked Blends. The cross-linked samples prepared by the steps described above were allowed to swell in toluene to estimate the degree of polymerization between cross-links, N_c . According to the Flory-Rehner theory¹⁴ of swelling, the degree of polymerization between cross-links can be calculated from the equation

$$\ln(1 - \varphi) + \varphi + \chi_1 \varphi^2 + \frac{v_1}{\nu m N_c} (\varphi^{1/3} - \frac{\varphi}{2}) = 0 \quad (1)$$

where φ is the volume fraction of the network, v_1 is the molar volume of solvent, ν is the specific volume of the polymer, m is the molecular weight of the polymer repeat unit, and χ_1 is the Flory interaction parameter between polymer and solvent. The cross-linked samples were disk-shaped, 14 mm in diameter and 1 mm in thickness, before the swelling. Swelling ratios, Q , were calculated from the measured value of the disk diameter and the thickness after the samples had reached swelling equilibrium. Swelling ratios are presented in Table II. The inverse of the swelling ratio can then be used in eq 1 ($\varphi = 1/Q$). The molar volume of toluene is 106.3 cm³/mol. The specific volume used for the blend, 1.056 cm³/g, was taken as the average value of DPB and HPB. A weighted average value of the molecular weight of deuterated butadiene monomer and that of protonated butadiene monomer was calculated and used in eq 1 as the monomeric molecular weight. The value of the interaction parameter between HPB and toluene used was 0.465 as reported by Sasaki et al.¹⁵ The obtained values of N_c are given in Table II.

3. SANS Measurements. The SANS experiments were carried out by using the 30-m SANS instrument at the NIST Cold Neutron Research Facility. In this study, pinhole collimation was used with a 7-Å neutron wavelength. The wavelength resolution, $\Delta\lambda/\lambda$, was 0.21, where λ is the wavelength of the neutron

beam and $\Delta\lambda$ is the full width at half-maximum (fwhm). A two-dimensional detector with a sample-to-detector distance of 15.30 m was used. The observed scattering intensity was corrected for electronic background, sample transmittance and thickness, empty sample cell scattering, and detector inhomogeneity. The intensity was then converted to absolute units with a deuterated polystyrene (DPS) and polystyrene (HPS) blend (50/50 wt %), which was calibrated using a silica gel secondary standard on the NIST 8-m SANS.¹⁶ The corrected scattered intensity was then circularly averaged to obtain the dependence of scattering intensity on wave vector [$q = (4\pi/\lambda) \sin(\theta/2)$, θ being the scattering angle].

A copper heating block was used to control the specimen temperature to within ± 0.2 °C of the desired temperature during measurements. Specimens were held at temperature at least for 30 min before the SANS measurements were started.

III. Results and Discussion

1. Simple Discussion of Linear Blend Scattering. De Gennes has calculated the scattering function, $I_L(q)$, of a binary polymeric mixture in the single-phase state based on the random-phase approximation (RPA) in the context of the mean-field model.¹⁷ It has been shown in many publications^{3-7,18-21} that the RPA calculation describes the scattering intensity of polymer mixtures quite well in the single-phase region of the phase diagram. For the asymmetric polymer pair it is given by

$$\left[\frac{I_L(q)}{k_N} \right]^{-1} = \frac{1}{N_A \phi_A \nu_A G_D(X_A)} + \frac{1}{N_B \phi_B \nu_B G_D(X_B)} - \frac{2\chi}{\nu_0} \quad (2)$$

where N_K , ϕ_K , ν_K , $G_D(X_K)$, and χ are, respectively, the degree of polymerization, the volume fraction, the monomeric molecular volume, the Debye scattering function of a single Gaussian coil for polymer K [$K = A$ or B , $G_D(X_K) = (2/X_K^2)[X_K - 1 + \exp(-X_K)]$], and the Flory interaction parameter per monomeric unit. k_N is the contrast factor for neutrons, which can be written as

$$k_N = N_0(b_A/\nu_A - b_B/\nu_B)^2 \quad (3)$$

with b_K as the scattering length of one monomeric unit of polymer K and N_0 as Avogadro's number. ν_0 is the reference cell volume, which is given by

$$\nu_0 = (\phi_A/\nu_A + \phi_B/\nu_B)^{-1} \quad (4)$$

and X_K is defined as

$$X_K = q^2 R_{gK}^2 = q^2 (N_K a_K^2 / 6) \quad (5)$$

where R_{gK} is the unperturbed radius of gyration and a_K is the statistical segment length of polymer K . The scattering function calculated from eq 2 is a monotonically decreasing function of q .

In the following section (III-2) eq 2 was applied to the un-cross-linked (linear) DPB/HPB blend to obtain χ as a function of temperature T , $\chi(T)$, and the spinodal temperature, T_s .

2. Characterization of Un-Cross-Linked (Linear) Blend in the Single-Phase State. SANS measurements for the DPB/HPB blend in the single-phase region of the phase diagram have been done as a function of temperature (T). Figure 1 shows a plot of SANS profiles of the un-cross-linked blend (hereafter referred to as the linear blend) as a function of q at different temperatures. Note that the SANS profiles have been put onto an absolute intensity scale. The vertical lines for each symbol in the figure are error bars. It is important to point out that the accuracy of all SANS data was within $\pm 1.5\%$. The scattered intensity increased with decreasing temperature,

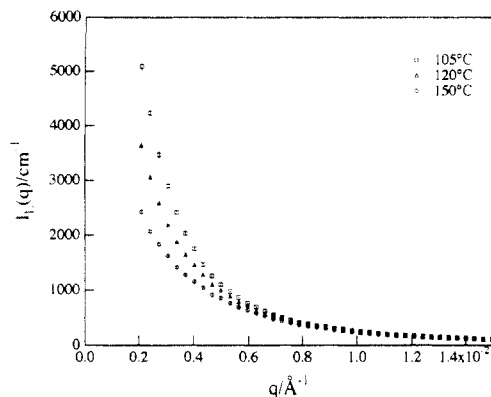


Figure 1. SANS profiles of DPB/HPB un-cross-linked (linear) blend ($\phi_{\text{DPB}} = 0.465$; critical composition) at various temperatures in the single-phase state.

indicating that the DPB/HPB blend is an UCST-type system.

Nonlinear regression fitting⁴ of the SANS profiles to eq 2 was done to determine χ as a function of T . The detailed fitting procedure can be found elsewhere.¹² Since the objective of this paper is not a full characterization of the DPB/HPB blend, the detailed analysis of the DPB/HPB blend (e.g., composition dependence of χ) will be presented in a separate publication.¹² The temperature dependence of χ is given by

$$\chi = -5.34 \times 10^{-4} + 0.314/T \quad (6)$$

with the spinodal temperature being 99.2 °C. It should be noted that the χ value at the spinodal point (χ_s) was calculated to be 3.10×10^{-4} .

3. Small-Angle Neutron Scattering from Cross-Linked Blends. A. Theory for Cross-Linked Polymer Blends. De Gennes has given in a short paper a theoretical investigation on the effect of A-B cross-links on concentration fluctuations and the phase diagram for a miscible A/B polymer blend.²² There are some assumptions in his theory: (i) the blend is cross-linked randomly with A-B cross-links (exclusively) to produce a network but the presence or absence of A-A or B-B cross-links should not change the results, at least qualitatively; (ii) the starting blend is symmetric ($N_A = N_B = N$, $\phi_A = \phi_B = 0.5$); (iii) $N_c \ll N$ to assure the system is not close to the gel point. We believe that the peroxide cross-linking reaction results in random cross-linking of the DPB/HPB system. In addition, the DPB/HPB blend used in this study was close to a symmetric blend (see Table I), giving rise to a closely symmetric cloud point curve.¹² N_c was on the order of 10 times smaller than the degree of polymerization of the HPB, which is the shorter of the two components (see Tables I and II). Writing the free energy in terms of its Fourier components allows the evaluation of the structure factor, $S_c(q)$, for the system in the single-phase state. $S_c(q)$ is given by

$$S_c(q)^{-1} = \frac{C}{q^2} + \frac{1}{2}(\chi_s - \chi) + \frac{a^2 q^2}{24} \quad (7)$$

where χ_s is the χ value at the critical point for the un-cross-linked linear blend, a is the statistical segment length of the polymer chains ($a_A = a_B = a$), and C is related to the "internal rigidity" of the chains. According to de Gennes $C \approx 36/(N_c^2 a^2)$.

$S_c(q)$ as described in eq 7 has a scattering maximum at a nonzero q vector (termed q^*), in contrast to the scattering function for an un-cross-linked polymer blend, $I_L(q)$, which has an maximum at $q = 0$. The scattering maximum in

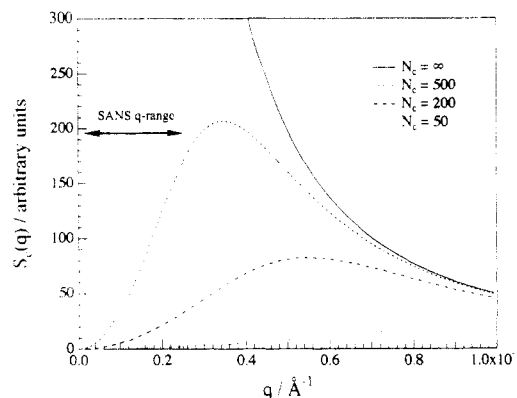


Figure 2. Plots of the structure factor $S_c(q)$ vs q given by eq 7 for four different cross-link densities ($N_c = \infty, 500, 200, 50$). Parameters of $a = 7 \text{ \AA}$, $\chi_s = 0$ (corresponding to infinite molecular weight of the starting blend), and $\chi = 0.0001$ are used in eq 7.

$S_c(q)$ can be understood by noting that $S_c(q = 0) = 0$ in eq 7, which is because the chains are cross-linked to each other so that there is no Fourier mode of the concentration fluctuations with infinite wavelength (i.e., zero osmotic compressibility) and because the system is assumed to have zero isothermal compressibility. As the value of χ approaches the critical value χ_c for the cross-linked blend, the peak in the structure factor increases in intensity until it diverges at $\chi = \chi_c$. This is the mean-field spinodal point for the cross-linked blend. It is interesting to note that this prediction is very similar to that for block copolymers.²³

The position of the scattering maximum in $S_c(q)$ can be calculated from taking $\partial(S_c(q)^{-1})/\partial q = 0$ and solving for $q = q^*$

$$q^* = 5.42/(N_c^{1/2} a) \quad (8a)$$

$$q^* = 2.21 R_{gc}^{-1} \quad (8b)$$

where R_{gc} is the radius of gyration of the chain between cross-links. q^* scales inversely with R_{gc} and in general eq 8 can be rewritten as $q^* \sim (\text{const}) R_{gc}^{-1}$. Briber and Bauer have, on the other hand, reported 2.30 instead of 5.42 for the constant in eq 8a in their publication, in which they cross-linked a miscible polymer blend of deuterated polystyrene (DPS) and poly(vinyl methyl ether) (PVME) with γ -ray irradiation.⁹ In their case eq 8 can be rewritten as

$$q^* = 2.30/(N_c^{1/2} a) \quad (9)$$

Figure 2 represents the calculated structure factor from eq 7 for the cross-linked blends with $N_c = \infty$ (linear blend), 500, 200, and 50. In Figure 2, q^* increases as N_c decreases. It should be emphasized in the figure that a large suppression in the scattered intensity due to the cross-links is expected to occur in the small q regime covered in our experiment, as a consequence of the elastic effect of the network on the thermal concentration fluctuations. Note that the smaller the value N_c (the tighter the network), the larger the suppression.

Following either the prediction of de Gennes (eq 8) or the reported value by Briber and Bauer (eq 9), one can calculate the q^* for the DPB/HPB blend system (Table II).

The estimated q^* 's from either eq 8 or 9 for the cross-linked blends are outside the experimental range ($1.5 \times 10^{-3} < q (\text{\AA}^{-1}) < 2.5 \times 10^{-2}$) except for the sample with $N_c = 446$ as calculated from eq 9. However, as is obvious

Table III
 χ_c and ϵ at 0 (ϵ_0) and 150 °C (ϵ_{150}) for DPB/HPB
Cross-Linked Blends

N_c	$\chi_c \times 10^2$ ^a	ϵ_0 ^b	ϵ_{150} ^b
446	1.13	0.945	0.981
167	2.96	0.979	0.993
98	5.04	0.988	0.996
38	12.8	0.995	0.998

^a Calculated from eq 10. ^b Calculated from eq 11.

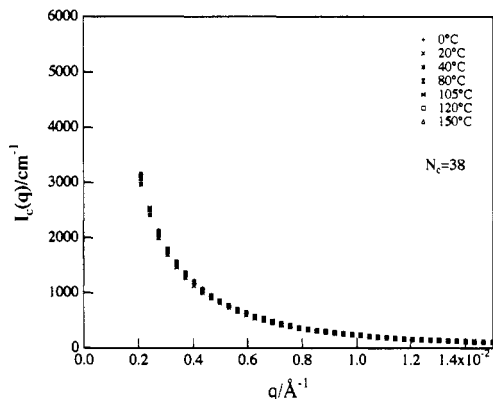


Figure 3. Plots of typical scattering curves, $I_c(q)$, for one of the cross-linked blends ($N_c = 38$) vs q .

from Figure 2, the effect of cross-linking on the scattering should be observed most effectively at q smaller than q^* , i.e., in the q range covered in our experiment, where a large suppression of the scattered intensity is expected after cross-linking the blend. Thus, the fact that the q range examined in this paper is smaller than the position of the calculated q^* does not invalidate the evaluation of the theory of de Gennes.

The value of $\chi = \chi_c$ at the critical point can be calculated from eq 7 by setting $S_c(q^*) = 0$.

$$\chi_c - \chi_s = 2(6)^{1/2}/N_c \quad (10)$$

Briber and Bauer reported an experimental value of 3.4 instead of $2(6)^{1/2}$ (≈ 4.9). These numbers were in agreement within the reported error bars due to the large extrapolations involved in determining T_s for the DPS/PVME system. χ_c values for DPB/HPB cross-linked blends were calculated from the theory of de Gennes and are presented in Table III, in which ϵ is defined later in eq 11.

B. SANS Scattering Profiles from Cross-Linked Polymer Blends. Figure 3 shows a plot of experimental SANS profiles of the cross-linked blend having $N_c = 38$ as a function of q vector. This cross-linked blend was chosen because this is the one having the smallest N_c , so that the largest suppression in the scattered intensity is expected.

The SANS measurements have been done in the temperature range from 0 to 150 °C, after the cross-linking at 150 °C as discussed (in section II-1). There are several particular features in Figure 3: (i) the scattering decreases monotonically with q vector; (ii) the data were essentially temperature independent; (iii) the concentration fluctuations present at the temperature of cross-linking appear to be trapped by the cross-linking reaction; (iv) the cross-linked blends did not microphase separate even well below the critical temperature for the linear blend (down to 0 °C; $T_c = 99.2$ °C for the linear blend), suggesting that the cross-linking increased the single-phase region of the phase diagram and shifted down the critical temperature below 0 °C. These trends were observed for all of the cross-linked blends.

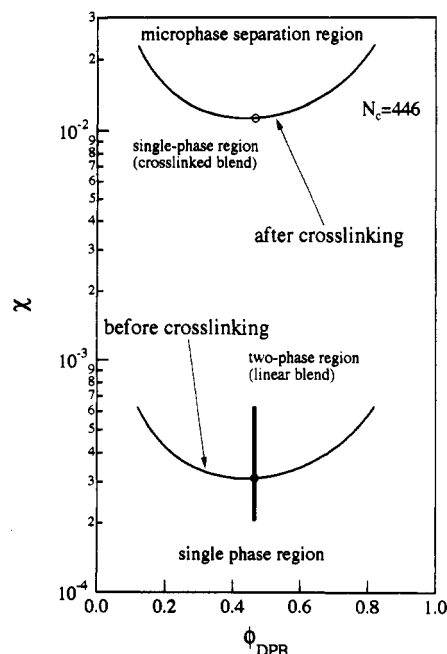


Figure 4. Predicted change of phase diagram for the DPB/HPB blend before and after the cross-linking ($N_c = 446$).

Feature iii was found to be obvious when we plotted the scattering profiles before and after cross-linking at 150 °C, although they are not shown in Figure 3. The two profiles turned out to be *almost* identical, as will be shown later implicitly in Figure 5, for example. Features i and iii may be inconsistent with the prediction made by de Gennes and are associated with the concentration fluctuations of the linear blends which are frozen-in by the cross-linking, i.e., the effect that was not included in the original theory of de Gennes, as will be discussed later in the text in detail (section III-4). Feature iv is consistent with the prediction by de Gennes.

Combined with the conclusions obtained from feature iv, feature ii may be interpreted as a consequence that the critical temperature was shifted down far below 0 °C, so that the thermodynamic state of the cross-linked blend stays unchanged over the temperature range covered in our experiment. Then the first question we would like to address is why our system after the cross-linking is in the single-phase state far from the critical point. This situation may be realized in the following analysis.

Using Eq 10, the χ values at the critical point for the cross-linked blends (χ_c) were calculated for different values of N_c . We can also calculate a reduced interaction parameter, ϵ , for the cross-linked blends which is defined by

$$\epsilon = (\chi_c - \chi)/\chi_c \quad (11)$$

ϵ reflects how far the system is from the critical point. Table III shows various calculated ϵ values for the cross-linked blends. In Table III, ϵ_0 and ϵ_{150} denote the value of ϵ at 0 and 150 °C, respectively. It should be noted that ϵ at 150 °C for the linear blend was 0.329, indicating that the great increase in the calculated value of ϵ is theoretically expected after the cross-linking. The fact that ϵ is close to unity implies that the cross-linked blend is expected to be in the single-phase state very far from the critical point. It is obvious from Table III that ϵ is expected not to change much (at most 5% change), although the SANS measurements were made over a wide range of temperature.

Figure 4 illustrates the effect of the cross-linking on the phase diagram predicted by the theory of de Gennes. The phase diagram correctly indicates the prediction only at

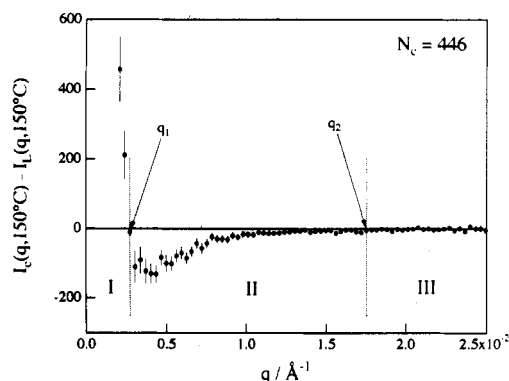


Figure 5. Subtracted scattering intensity $I_c(q, 150\text{ }^{\circ}\text{C}) - I_L(q, 150\text{ }^{\circ}\text{C})$ vs q for the cross-linked blend ($N_c = 446$). Two crossover wave vectors (q_1 and q_2) are shown.

the critical composition $\phi_{\text{DPB}} = 0.466$, while the rest of the spinodal line for the cross-linked blend is only schematic. The diagram after the cross-linking is obtained for the cross-linked blend with $N_c = 446$. The lower solid line represents the experimentally determined spinodal line for the linear blend.¹² Although we could not experimentally determine T_c for the cross-linked blends, we still can estimate T_c 's according to the theory of de Gennes. The higher solid line shows the calculated spinodal line using eq 10 for the cross-linked blend. Once the cross-links are introduced to the DPB/HPB blend, the size of the single-phase region increases, which is consistent with the experimental results. Since χ is inversely proportional to T , the UCST-type phase diagram shifts down along the temperature axis with cross-linking.

The height of the symbol on the phase diagram (small vertical solid line across the spinodal line before cross-linking) represents the change in χ with the change of temperature between 0 and 150 $^{\circ}\text{C}$, which is estimated from $\chi(T)$ measured for the linear blend (eq 6). The small change in ϵ is obvious in Figure 4. In addition, it is also clear that the actual temperature range is far from the phase boundary of the cross-linked blend.

4. Comparison of Cross-Linked Blends and Linear Blends at the Cross-Linking Temperature. It is important to compare the scattering curves for the cross-linked blends, $I_c(q)$, with that for the linear blend, $I_L(q)$, at the temperature of cross-linking because the effect of cross-links on the scattering can be directly observed by comparing the scattering profiles before and after cross-linking at the cross-linking temperature of 150 $^{\circ}\text{C}$. To clearly see the effect, we subtracted $I_L(q, 150\text{ }^{\circ}\text{C})$ from $I_c(q, 150\text{ }^{\circ}\text{C})$, where $I_L(q, 150\text{ }^{\circ}\text{C})$ and $I_c(q, 150\text{ }^{\circ}\text{C})$ denote, respectively, the scattering for the linear blend and the crosslinked blend at 150 $^{\circ}\text{C}$.

Figure 5 shows the plot of $I_c(q, 150\text{ }^{\circ}\text{C}) - I_L(q, 150\text{ }^{\circ}\text{C})$ vs q for the specimen with $N_c = 446$ at 150 $^{\circ}\text{C}$. Error bars are attached to the data points, which clearly demonstrate that the difference between $I_c(q, 150\text{ }^{\circ}\text{C})$ and $I_L(q, 150\text{ }^{\circ}\text{C})$ is significant at low q . As already mentioned in section III-3, notable deviations from $I_L(q, 150\text{ }^{\circ}\text{C})$ cannot be observed at q larger than $0.02\text{ }\text{\AA}^{-1}$, which substantiate the choice of q range covered in our experiment. As indicated in the figure by arrows, two different crossover wavenumbers q_1 and q_2 were found. At q vectors smaller than q_1 ($q < q_1$; regime I), $I_c(q, 150\text{ }^{\circ}\text{C}) - I_L(q, 150\text{ }^{\circ}\text{C})$ has positive values. On the other hand, at q vectors larger than q_1 but smaller than q_2 ($q_1 < q < q_2$; regime II), $I_c(q, 150\text{ }^{\circ}\text{C}) - I_L(q, 150\text{ }^{\circ}\text{C})$ has negative values; i.e., the scattering was suppressed after cross-linking.²⁵ In addition, at q vectors larger than q_2 ($q > q_2$; regime III), $I_c(q,$

$150\text{ }^{\circ}\text{C}) - I_L(q, 150\text{ }^{\circ}\text{C})$ is approximately zero, implying that at length scales smaller than that corresponding to q_2^{-1} there was no effect of cross-linking on the scattering curve. It might be expected that at q vectors larger than the inverse of the network mesh size the scattering would be similar to that of the un-cross-linked blend, but it is difficult, within the precision of this experiment, to correlate the value of q_2 directly or quantitatively with the mesh size of the cross-linked network, i.e., $N_c^{1/2}a$.

In this study the cross-linking was induced by a temperature jump from 105 to 150 $^{\circ}\text{C}$, and the following two competing processes should exist during the cross-linking at 150 $^{\circ}\text{C}$: (i) the cross-linking reaction rate, R_c , and (ii) the q -dependent relaxation rate of the concentration fluctuations in the single-phase state, Γ_q (for the linear blend before cross-linking). In other words, when the cross-linking reaction tries to lock-in the concentration fluctuations present in the blend, these fluctuations try to relax. Note Γ_q increases with increasing q .

The wavelength $\Lambda_1 (=2\pi/q_1)$ is defined as a crossover wavelength or the wavenumber q_1 as a crossover wavenumber at which $R_c = \Gamma_q$. In regime I where $q < q_1$, R_c is considered to be faster than Γ_q ($R_c > \Gamma_q$). Hence, the concentration fluctuations having a wavelength longer than Λ_1 or a wavenumber smaller than q_1 can be effectively frozen-in by the cross-linking reaction. In this sense, the position of the wave vector q_1 reflects the reaction rate of the cross-linking, i.e., $R_c \approx \Gamma_{q_1}$. To lock-in the concentration fluctuations at a larger q_1 requires a faster cross-linking (larger R_c) because of the faster relaxation rate, Γ_q . If the concentration fluctuations in the linear blend are fixed and maintained in the cross-linked blend in regime I, we expect that $I_c(q) - I_L(q) \approx 0$. However, actually, we found that $I_c(q) > I_L(q)$, as seen in Figure 5. This can be interpreted as follows. Even a relatively short transient time required for the temperature jump may produce appreciable cross-linking below 150 $^{\circ}\text{C}$. This indicates locking-in of the concentration fluctuations at $T \leq 150\text{ }^{\circ}\text{C}$. The concentration fluctuations frozen-in at $T \leq 150\text{ }^{\circ}\text{C}$ give rise to the scattered intensity $I_c(q)$ higher than $I_L(q)$ at 150 $^{\circ}\text{C}$, which may explain the experimental observation of $I_c(q) > I_L(q)$.

On the other hand, in regimes II and III, R_c is slower than Γ_q ($R_c < \Gamma_q$). The concentration fluctuations in this q range have shorter wavelength than Λ_1 and hence faster relaxation rate than R_c . Thus, the concentration fluctuations are able to relax before being fixed by the cross-linking reaction. In regime II the wavelength Λ ($\Lambda = 2\pi/q$) is larger than or comparable to the mesh size of the network. We propose the following interpretation for the suppression of the scattered intensity occurred after cross-linking in this regime. The scattered intensity after the cross-linking, $I_c(q)$, is approximated by

$$I_c(q) \approx S_c(q) + S_f(q) \quad (12)$$

where $S_f(q)$ is the scattering from the frozen-in thermal concentration fluctuations of the linear blend at the time when the cross-linking took place and $S_c(q)$ is the scattering from the cross-linked blend given by de Gennes (eq 7). Figure 6 shows the schematic illustration of our explanation for the suppression of the scattering due to the cross-linking. The scattering from the thermal concentration fluctuations in the linear blend before the cross-linking, $I_L(q)$, should be suppressed to the level of $S_c(q)$ in Figure 6a, if there is no contribution from $S_f(q)$, as is the case treated by de Gennes. In this case $I_c(q) - I_L(q)$ would be $S_c(q) - I_L(q)$ in Figure 6b because this is the ideal case in which $I_c(q) = S_c(q)$. However, there is always the

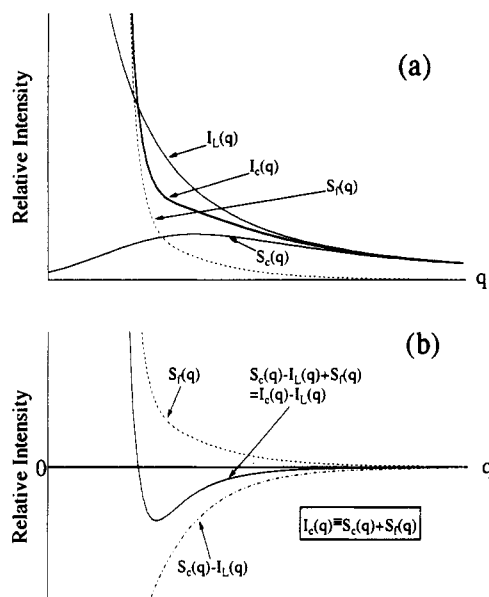


Figure 6. Schematic illustration of the effect of the frozen-in concentration fluctuations at cross-linking, $S_f(q)$, on the observed scattering intensity profile, $I_c(q)$ (a), and on the intensity difference of $I_c(q) - I_L(q)$ (b).

contribution from $S_f(q)$ which is shown by the dashed line in Figure 6b. In reality, $I_c(q) - I_L(q)$ is the solid line in Figure 6b because of the presence of the frozen-in concentration fluctuations. Hence, the observed scattering intensity, $I_c(q)$, is suppressed as shown in Figure 6a. That is, the suppression predicted by de Gennes is masked by the scattering from the frozen-in concentration fluctuations. This also explains the experimental fact that no significant suppression of the scattered intensity occurred after cross-linking, which is feature iii in section III-3. Therefore, it is crucial to note that the frozen-in concentration fluctuations at 150 °C are important and are the effect that was not included in the original theory of de Gennes.

As already discussed in section III-3 and Figure 4, the reduced interaction parameter, ϵ , is expected to change at most 5% (Table III). $S_c(q)$ depends on χ and T ; the closer the system to the critical point χ_c or T_c , the higher the intensity. On the other hand, $S_f(q)$ may be essentially fixed and independent of χ or T . The small change in ϵ gives a small change in $S_c(q)$ which should be masked by $S_f(q)$ from the frozen-in concentration fluctuations. This explains feature ii in section III-3 found experimentally, i.e., the scattering curves $I_c(q)$ were essentially independent of temperature.

In regime III where $q > q_2$, $R_c \ll \Gamma_q$, the cross-linked blend behaves similarly to the un-cross-linked blend because the size scales probed may be smaller than the mesh size of the network.

Figure 7 is a plot of q_1 vs N_c . It can be seen that q_1 decreases with increasing N_c . Since N_c is inversely related to the amount of peroxide in the system, the larger the N_c , the smaller the amount of peroxide and the smaller the R_c . With a smaller R_c , the concentration fluctuations with longer wavelengths (hence having the slower relaxation rate) can relax. Therefore, Λ_1 should increase (or q_1 should decrease) as N_c increases. This is consistent with the data in Figure 7.

The crossover vectors q_2 are also plotted as a function of N_c in Figure 7. There is a lot of scatter in the data, making it difficult to draw any conclusions as to the dependence of q_2 on N_c .

5. Comparison of DPB/HPB System and DPS/PVME System. It is worth considering the reason why

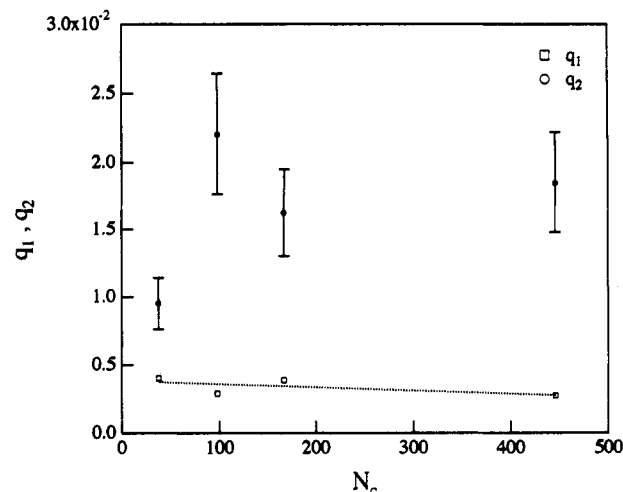


Figure 7. Plots of crossover wave vectors q_1 and q_2 vs N_c . The dotted line is a visual guide.

Table IV
 χ_c and ϵ (120 and 180 °C) for DPS/PVME Cross-Linked Blends^a

N_c	$\chi_c \times 10^3$ ^b	ϵ_{120}^c	ϵ_{180}^c
870	3.92	1.87	0.0979
440	7.74	1.44	0.543
180	1.89	1.18	0.813

^a $\chi_{120} = -3.40 \times 10^{-3}$, $\chi_{180} = 3.54 \times 10^{-3}$ for DPS/PVME blend.
^b Calculated from eq 10. ^c Calculated from eq 11.

$I_c(q)$ for the DPB/HPB system decreases monotonically with q vector (i.e., no scattering maximum in $I_c(q)$ or no tendency of increasing $I_c(q)$ with increasing q is observed over the q range in our experiments), while Briber and Bauer observed a scattering maximum in $I_c(q)$ for their PSD/PVME system.⁹ In Table IV the χ values at the spinodal temperature for the DPS/PVME system are presented together with the calculated ϵ at 120 and 150 °C for different cross-link densities. In calculating ϵ the following experimentally determined relationship for the DPS/PVME un-cross-linked blend was used.²⁴

$$\chi = 4.9 \times 10^{-2} - 20.6/T \quad (13)$$

Although ϵ values change, at most, a couple of percent for DPB/HPB cross-linked blends over the temperature range 0–150 °C, the ϵ values for DPS/PVME cross-linked blends change as much as 20 times over the temperature range 120–180 °C. This is because the temperature dependence of the χ parameter for the DPS/PVME blend is much stronger than that for the DPB/HPB blend, e.g., the absolute value of the coefficient in the second term of eq 13 for the DPS/PVME blend was 20.6, while that for the DPB/HPB blend was only 0.314 (see eq 6). Therefore, even for measurements over the same temperature range, the change in the χ value will be much larger in the case of DPS/PVME than in the case of DPB/HPB.

The striking difference between the two sets of data in terms of the presence (DPS/PVME) or the absence (DPB/HPB) of the scattering maximum can be understood by taking into consideration the effect of frozen-in concentration fluctuations during the cross-linking (see Figure 6). In both the γ -ray cross-linked DPS/PVME blend and the peroxide cross-linked DPB/HPB blend, the concentration fluctuations present in the blends at the curing temperature were frozen. Then when the phase boundary is approached, the predicted scattering $S_c(q)$ is superimposed on top of the scattering $S_f(q)$ from the frozen-in concentration fluctuations. In case of DPS/PVME cross-linked blends, the change in χ with temperature results

in a significant change in the concentration fluctuations in comparison with the frozen fluctuations, and at temperatures close to the critical temperature, the contribution of the scattering from the concentration fluctuations $S_c(q)$ dominates $S_f(q)$ from the frozen-in fluctuations. That is, in Figure 6, $S_c(q) - I_L(q)$ becomes bigger as the phase boundary is approached so that there is no longer the negative part in $I_c(q) - I_L(q)$. Hence, the peak in $I_c(q)$ could be observed. The essential difference between the two systems is how close the system is to the phase boundary and the relative change in χ over the temperature range covered in the experiments. This factor changes $S_c(q) - I_L(q)$ relative to $S_f(q)$, which can explain the presence and the absence of the scattering peak in $I_c(q)$.

It should be noted that the small χ range covered in this experiment is typical of what is available in many polymer systems with small B coefficient ($\chi = A + B/T$) and that DPS/PVME is more the exception than the rule, as the B value for DPS/PVME is abnormally large.

IV. Conclusion

Small-angle neutron scattering experiments have been done to study the effect of peroxide cross-linking on the phase diagram and the scattering for a critical mixture of DPB and HPB. It was observed that the scattering profiles for the cross-linked blends were monotonically decreasing with increasing q and essentially temperature independent. It was also found that the cross-linked blends remained single phase even at temperatures 100 °C below the critical temperature for the linear blend, suggesting a large increase of the single-phase region of the phase diagram caused by cross-linking. An attempt has been made to compare these findings with the theory for such a system that has been published by de Gennes.²² The effect of cross-links on the phase diagram for a polymer blend is estimated on the basis of the theory, and the result is shown in Figure 4.

A comparison between the results of the DPB/HPB system and those of the DPS/PVME system reported by Briber and Bauer has also been made. It was shown that the temperature dependence of the χ parameter for the DPB/HPB system is much smaller than that for the DPS/PVME system, which plays an important role in explaining the absence of the predicted peak in the scattering curve.

The effect of the frozen-in concentration fluctuations present in the blend during cross-linking is found to be an extremely important factor in determining the structure factor for the cross-linked blends, especially at temperatures far from the critical point in the single-phase state, although the theory of de Gennes does not take this factor into account.

By comparison of the scattering before and after the cross-linking at the cross-linking temperature, the presence of a suppression in the scattering after cross-linking was observed. This suppression in the scattering was predicted by the theory of de Gennes. Two crossover wave vectors, q_1 and q_2 were defined. q_1 and q_2 are thought to be related to the reaction rate of the cross-linking and possibly the mesh size of the cross-linked network, respectively.

Acknowledgment. We are grateful to Dr. Barry J. Bauer for valuable discussions. We are grateful to Nippon Zeon Co. for providing the HPB sample. This work is supported in part by a Grant-in-Aid for Scientific Research in Priority Areas ("New Functionality Materials Design, Preparation and Control") from the Ministry of Education, Science and Culture, Japan.

References and Notes

- (1) Matsuo, M.; Nozaki, C.; Jyo, Y. *Polym. Eng. Sci.* **1969**, *9*, 197.
- (2) Olabisi, O.; Robeson, L. M.; Shaw, M. T. *Polymer-Polymer Miscibility*; Academic Press: New York, 1979.
- (3) Han, C. C.; Bauer, B. J.; Clark, J. C.; Muroga, Y.; Matsushita, Y.; Okada, M.; Tran-Cong, Q.; Chang, T.; Sanchez, I. *Polymer* **1988**, *29*, 2002.
- (4) Shibayama, M.; Yang, H.; Stein, R. S.; Han, C. C. *Macromolecules* **1985**, *18*, 2179.
- (5) Bates, F. S.; Wignall, G. D.; Koehler, W. C. *Phys. Rev. Lett.* **1985**, *55*, 2425.
- (6) Bates, F. S.; Dierker, S. B.; Wignall, G. D. *Macromolecules* **1986**, *19*, 1938.
- (7) Bates, F. S.; Muthukumar, M.; Wignall, G. D.; Fetters, L. J. *J. Chem. Phys.* **1988**, *21*, 535.
- (8) Olvera de la Cruz, M.; Sanchez, I. C. *Macromolecules* **1986**, *19*, 2501.
- (9) Briber, R. M.; Bauer, B. J. *Macromolecules* **1988**, *21*, 3296.
- (10) Hashimoto, T.; Takenaka, M.; Jinnai, H. *Polym. Commun.* **1989**, *30*, 177.
- (11) Flory, P. J. *J. Chem. Phys.* **1941**, *9*, 660. Higgins, M. L. *J. Chem. Phys.* **1941**, *9*, 440.
- (12) Jinnai, H.; Hasegawa, H.; Hashimoto, T.; Han, C. C. Unpublished results.
- (13) Hashimoto, T.; Izumitani, T.; Takenaka, M. *Macromolecules* **1989**, *22*, 2293. If the samples stored at room temperature have large phase-separated domains, they should be kept at 105 °C for a very long time before they are homogenized to a single phase. The time required is estimated to be $R^2/6D$, where D is the mutual diffusivity and R is the maximum domain size. Thus, the mechanical mixing accelerates and assures homogenization of the mixtures to single phase at 105 °C.
- (14) Flory, P. J.; Rehner, J., Jr. *J. Chem. Phys.* **1943**, *11*, 521.
- (15) Sasaki, K.; Hashimoto, T. *Macromolecules* **1984**, *17*, 2818.
- (16) Glinka, C. J.; Rowe, J. M.; LaRock, J. G. *J. Appl. Crystallogr.* **1986**, *19*, 427.
- (17) de Gennes, P.-G. *Scaling Concepts in Polymer Physics*; Cornell University Press: New York, 1979. de Gennes, P.-G. *J. Chem. Phys.* **1980**, *72*, 4756.
- (18) Sakurai, S.; Hasegawa, H.; Hashimoto, T.; Han, C. C. *Macromolecules* **1990**, *23*, 451.
- (19) Hasegawa, H.; Sakurai, S.; Takenaka, M.; Hashimoto, T.; Han, C. C. *Macromolecules* **1991**, *24*, 1813.
- (20) Sakurai, S.; Jinnai, H.; Hasegawa, H.; Hashimoto, T.; Han, C. C. *Macromolecules* **1991**, *24*, 4839.
- (21) Sakurai, S.; Izumitani, T.; Hasegawa, H.; Hashimoto, T.; Han, C. C. *Macromolecules* **1991**, *24*, 4844.
- (22) de Gennes, P.-G. *J. Phys. (Paris)* **1979**, *40*, L-69.
- (23) Leibler, L. *Macromolecules* **1980**, *13*, 1602.
- (24) Briber, R. M.; Bauer, B. J. Unpublished data.
- (25) To induce the cross-linking, temperature is rapidly changed from 105 to 150 °C. Even a relatively short transient time between 105 and 150 °C may produce appreciable cross-linking below 150 °C (e.g., at 145 °C). If this effect is important, one should subtract $I_L(q)$ at T somewhat lower than 150 °C from the observed intensity $I_c(q)$ after the cross-linking. Since $I_L(q)$ at $T < 150$ °C is greater than that at 150 °C, the negative value $I_c(q) - I_L(q)$ becomes even greater than the estimated value based upon $I_L(q)$ at 150 °C, which is shown in Figure 5. Thus, the suppression of the intensity $|I_c(q) - I_L(q)|$ as estimated in Figure 5 may be a lower limit of the actual suppression. Thus, we think the differences $[I_c(q) - I_L(q)]$ are significant and support qualitatively the effects of cross-links predicted by de Gennes.